Journal Pre-proof

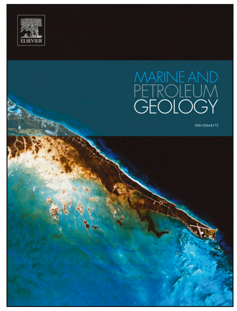

Gravity effects of fluid storage and withdrawal in a reservoir from 3D forward modelling

Paolo Mancinelli

PII: S0264-8172(21)00265-8

DOI: https://doi.org/10.1016/j.marpetgeo.2021.105162

Reference: JMPG 105162

To appear in: *Marine and Petroleum Geology*

Received Date: 28 January 2021

Revised Date: 17 May 2021

Accepted Date: 18 May 2021

Please cite this article as: Mancinelli, P., Gravity effects of fluid storage and withdrawal in a reservoir from 3D forward modelling, *Marine and Petroleum Geology*, https://doi.org/10.1016/j.marpetgeo.2021.105162.

Gravity effects of fluid storage and withdrawal in a reservoir from 3D forward modelling

Paolo Mancinelli – Dipartimento di Ingegneria e Geologia, Università G. D'Annunzio di Chieti-Pescara, Via dei Vestini 31, Chieti – Italy

Corresponding author: Paolo Mancinelli – paolo.mancinelli@unich.it

Keywords

Time variable gravity, Numerical modelling, Gas and hydrate systems.

Summary

The gravity effects of the possible reservoir scenarios after primary exploitation are tested in this work. Starting from the exploitable volume after primary hydrocarbon production of the very small and deep Volve field in the North Sea, we model several scenarios and calculate 3D forward gravity signatures accordingly. Namely, we test water flooding by aquifer rise, carbon dioxide storage, hydrogen storage using different cushion gases, hydrogen storage without cushion gas and hydrogen withdrawal. The differential gravity signature is calculated between two consecutive steps and the results provide detectability thresholds for each scenario. To evaluate effects of reservoir depth on the recovered gravity signatures, we repeat the calculations between 750 and 2750 m depth. Results of the modelling provide reference values for gravity signatures related to fluid storage in the worst-case scenario of a deep and thin (~100 m) reservoir and can provide valid constraints when mass loss estimation is required in leaking reservoirs. When the denser carbon dioxide and water are tested, these always provide detectable gravity signatures (> 3 μGal) even at the maximum modelled depth, whilst storage or withdrawal of hydrogen in the modelled depth range, often result in undetectable signatures.

Introduction

The investigation and monitoring of reservoirs using time-lapse gravity techniques have significantly evolved in the last decades thanks to improvements in gravimeters accuracy and data availability (e.g. Van Camp *et al*. 2017). New applications resulted in successful monitoring of fluid production or injection sites at large scales such the Prudhoe bay and North Sea sites (e.g. Hare *et al*. 1999; Eiken *et al*. 2000; Ferguson *et al*. 2007; Alnes *et al*. 2008; Eiken *et al*. 2008; Ferguson *et al*. 2008; Alnes *et al*. 2011) or at smaller scales (e.g. Jacob *et al*. 2010; Elliott and Braun, 2016; Mancinelli, 2020). Compared to forward or inverse gravity modelling techniques, where large-scale investigations are allowed by wide gravity anomaly datasets (e.g. Mancinelli *et al*. 2015; Dressel *et al.* 2018; Fedi *et al*. 2018; Mancinelli *et al*. 2019; 2020), time-lapse gravity requires acquisition of new high-precision data at each step of production/injection but allows detailed monitoring of fluid-related gravity changes.

In the frame of new environmental challenges driven by renewable energy exploitation and CO_2 sequestration, a few research projects have been recently developed to investigate the feasibility of geophysical monitoring of hydrogen and CO_2 storage sites through simulations over synthetic or real-case scenarios (Gasperikova and Hoversten, 2008; Pudlo *et al*. 2013; Hagrey *et al*. 2014; Kim *et al.* 2015; Krahenbul *et al.* 2015; Feldmann *et al*. 2016; Jacob *et al.* 2016; Pfeiffer *et al*. 2016; Kabuth *et al*. 2017; Wilkinson *et al.* 2017; Appriou *et al.* 2020; Goto *et al.* 2020; Kabirzadeh *et al.* 2020 and references therein). Among the proposed techniques, 3D gravity modelling successfully located gravity variations due to injection and withdrawal of hydrogen (Pfeiffer *et al*. 2016) or compressed air/gas (Hagrey *et al*. 2014) but differential gravity anomalies related to hydrogen storage and withdrawal was undetectable by modern gravimeters – i.e. time-lapse gravity anomalies were < 3 μGal (1 μGal = $1\text{x}10^{-8}$ m s^{-2}).

Despite several efforts aiming at the quantification of fluid storage gravity effects and their variations even in the long period (e.g. Appriou *et al.* 2020), the gravity signatures of different evolutive scenarios of a depleted reservoir were never addressed in a consequential modelling of each step considering all the possible fluids that can be temporarily or permanently stored. In fact, all the literature focused on single steps, either of injection or production and often considered only one fluid to be stored or withdrawn (mostly CO_2, more recently H_2). Similarly, the gravity effect of rising aquifer in the reservoir and how it relates to the signature of the stored fluid was never addressed. Moreover, the gravity signature of hydrogen storage or combined withdrawal with different cushion gases (CO_2 or N_2) is tested and compared for the first time in this work.

To address these questions and contribute in the discussion about differential gravity signatures related to fluid injection or production at reservoirs, we present a series of 3D forward calculations produced in a real, deep and very small reservoir representing the worst-case scenario for such tests. We model several possible scenarios after the production of the original hydrocarbons in place including the storage of CO_2 and storage and withdrawal of hydrogen. Furthermore, to evaluate contributions of the depth of the reservoir on the retrieved differential gravity signature, we repeat the same modelling with the reservoir depth ranging between 750 and 2750 m.

Data and Methods

Modelling is performed in the Volve field (Fig. 1) due to availability of production record and 3D geometrical model of the reservoir (Volve data village webpage). Located in the Central North Sea, the Volve field was discovered in 1993 and oil and gas production lasted between 2008 and 2016 with a total produced volume of $1.47\text{x}10^9$ Sm^3 (Sm^3 represents standard cubic meters at 15°C and $1010\text{x}10^2$ Pa). This volume includes the oil, gas, and formation water that have been produced (1.5 $\text{x}10^9$ Sm^3) and the injected water (0.03 $\text{x}10^9$ Sm^3). Ranging between 2750 and 3120 m depth, the reservoir is located in the Hugin Jurassic sandstones with an average reservoir thickness of ~100 m and porosity of 20% ±2.5 (Volve documentation included in the dataset). Given its size, depth and produced volumes (< 1.7×10^{9} Sm^{3}), the Volve field represents a very small and deep reservoir. Based on data included in the Volve dataset, the density of the produced hydrocarbons at reservoir conditions (3.28×10^{7} Pa and 106°C) is 710 kg m^{-3} (Volve documentation included in the dataset, see the reference list for a link to the web page hosting the dataset). The produced volumes over the eight years of activity at the Volve field, resulted in a gravity signature that was recently estimated to be ~-13 μGal (Mancinelli, 2020).

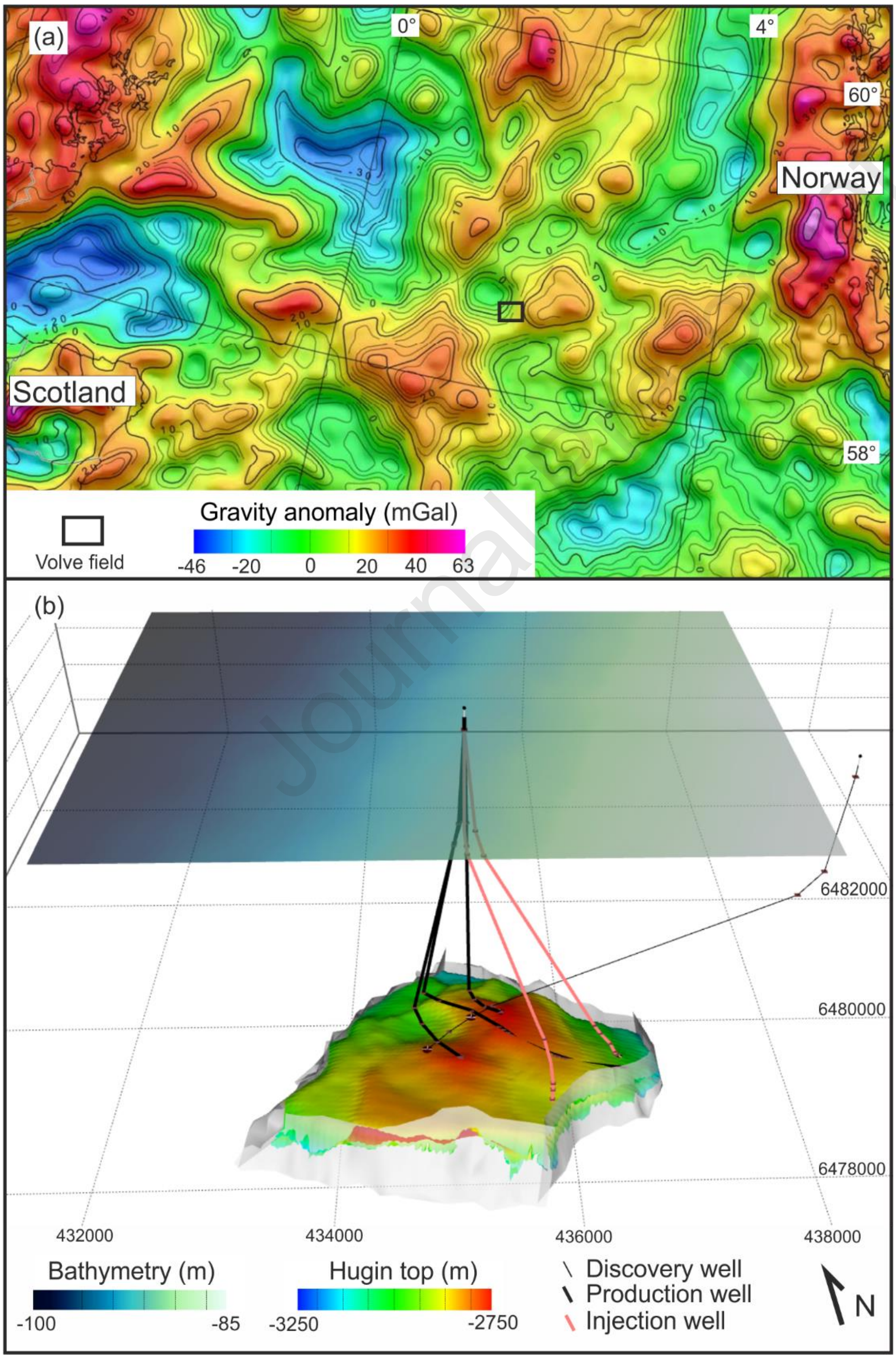

Figure 1. (a) Gravity anomalies over the study area, the free-air gravity anomaly at sea level and the Bouguer gravity anomaly on land (mod. from Olesen et al. 2010). (b) Perspective view of a 3D model of the Volve field (mod. from Mancinelli, 2020). Light grey surfaces in (b) represent bounding faults. Coordinates in (b) are in ED50 UTM 31N.

Through 3D forward models, we simulate the gravity effects of different evolutionary scenarios of the reservoir after primary production is completed. The possible cases are the following: (i) the reservoir can be used for CO_2 storage; (ii) the reservoir is flooded by water if strong aquifer push occurs; (iii) cushion gas is injected to eventually stabilize the aquifer and store hydrogen to be withdrawn when needed; (iiii) hydrogen is stored without cushion gas. We do not consider the usual scenario where hydrocarbons are stored in the reservoir because in this case the amplitude of the gravity effect would be the same as that obtained during production if no over-pressure is introduced. Similarly, we assume no displacement of those fluids that remained in the porous media after primary production, such fluids like residual hydrocarbons or irreducible water are assumed to not contribute in density changes of the reservoir volume. We also assume negligible surface deformation and porosity changes related to eventual pressure build-up in the surroundings of the injection point.

Modelling procedure

Forward 3D calculations are performed using the algorithm proposed by Li and Oldenburg (1998), where the vertical component of the gravity field due to density ρ(x,y,z) is given by:

$$g_z(r_0) = \gamma \int_V \rho(r) \frac{z - z_0}{|r - r_0|^3} \, dv$$

(1)

where V is the anomalous mass volume, $r_0 = (x_0, y_0, z_0)$ is the location of the observation point, $r = (x, y, z)$ locates the source and γ is the gravitational constant.

If we assume a constant density contrast within each prismatic cell of the 3D orthogonal mesh, the gravity field at the i^{th} observation point is given by

$$g_z(r_{0i}) = \sum_{j=1}^{M} \rho_j \left\{ \gamma \int_{\Delta V_j} \frac{z - z_0}{|r - r_{0i}|^3} \, dv \right\}$$

(2)

where ρ_j and ΔV_j are the anomalous density and volume of the j^{th} cell, respectively.

We discretize the reservoir volume using 25x25x25 m cubic cells (Fig. 2) and assuming sealing conditions at the faults bounding the Hugin sandstone. Finally, we homogenously distribute the mass variation due to gas injection or production within the entire reservoir volume that was left empty after the primary production.

Mass variations were computed considering the density of the modelled fluid (N_2, H_2O, CO_2 or H_2) at known or estimated pressure and temperature of the reservoir at each modelled depth. Table 1 shows the densities used for the modelling steps. Pressure and temperature data from the real reservoir at 2750 m depth were taken as a starting point to estimate the pressure and temperature conditions at the other modelled depths where measurements were not available. These estimates were produced assuming a ~1 × 10^7 Pa km^{-1} hydrostatic pressure gradient (Alnes *et al.* 2011) and a geothermal gradient of 26 °C km^{-1} (Volve documentation included in the dataset, see the reference list for a link to the web page hosting the dataset).

Depth (m)	P (x10^7 Pa)	T (°C)		N_2	H_2O	CO_2	H_2
2750	**3.28**	**106**	**Density (kg/m^3)**	247	968	671	18
			Status	Supercritical	Liquid	Supercritical	Supercritical
1750	**2.28**	**80**	**Density (kg/m^3)**	197	981	651	14
			Status	Supercritical	Liquid	Supercritical	Supercritical
750	**1.28**	**54**	**Density (kg/m^3)**	128	991	574	9
			Status	Supercritical	Liquid	Supercritical	Supercritical

Table 1. Density and status of the modelled fluids according to pressure and temperature at each depth, see text for discussion (NIST, 2016). Due to their supercritical status at these conditions, nitrogen, carbon dioxide and hydrogen show no distinct liquid or gas phases.

In the modelling procedure, we assume a homogeneous distribution of the mass variation within the entire reservoir. Thus, we calculate a mass variation induced by each operation on each cell according to the modelled volume occupied by the injected fluid or freed by the withdrawn fluid. Mass variation at each cell is provided by density contrast related to the inherited density of the cell at the end of the previous modelling step and the density of the fluid at the current modelling step. After 3D forward calculation, each injection or production step provides a positive or negative gravity signature, respectively. Finally, the differences between the maximum gravity observed after two consecutive steps, provide a differential gravity anomaly (Δg_z) useful to evaluate the detectability of the injection or withdrawal step. The detectability threshold for Δg_z is set to 3 μGal for onshore scenarios (Pfeiffer *et al.* 2016) and 6 μGal for offshore scenarios. However, these values represent conservative thresholds soon to be overcame because ~3 μGal-precision measures were achieved by Alnes *et al.* (2011) in the Sleipner offshore field, and ~2 μGal-precision onshore measures are achievable using superconducting gravimeters (Kim *et al.*, 2015).

To evaluate effects of reservoir depth on *Δg*$_z$, after modelling at the real depth of the Volve field (2750 m), we rigidly shift the reservoir 1000 m upward in the second step and 2000 m in the third step to run the same forward models at 1750 and 750 m depth, respectively (Fig. 2).

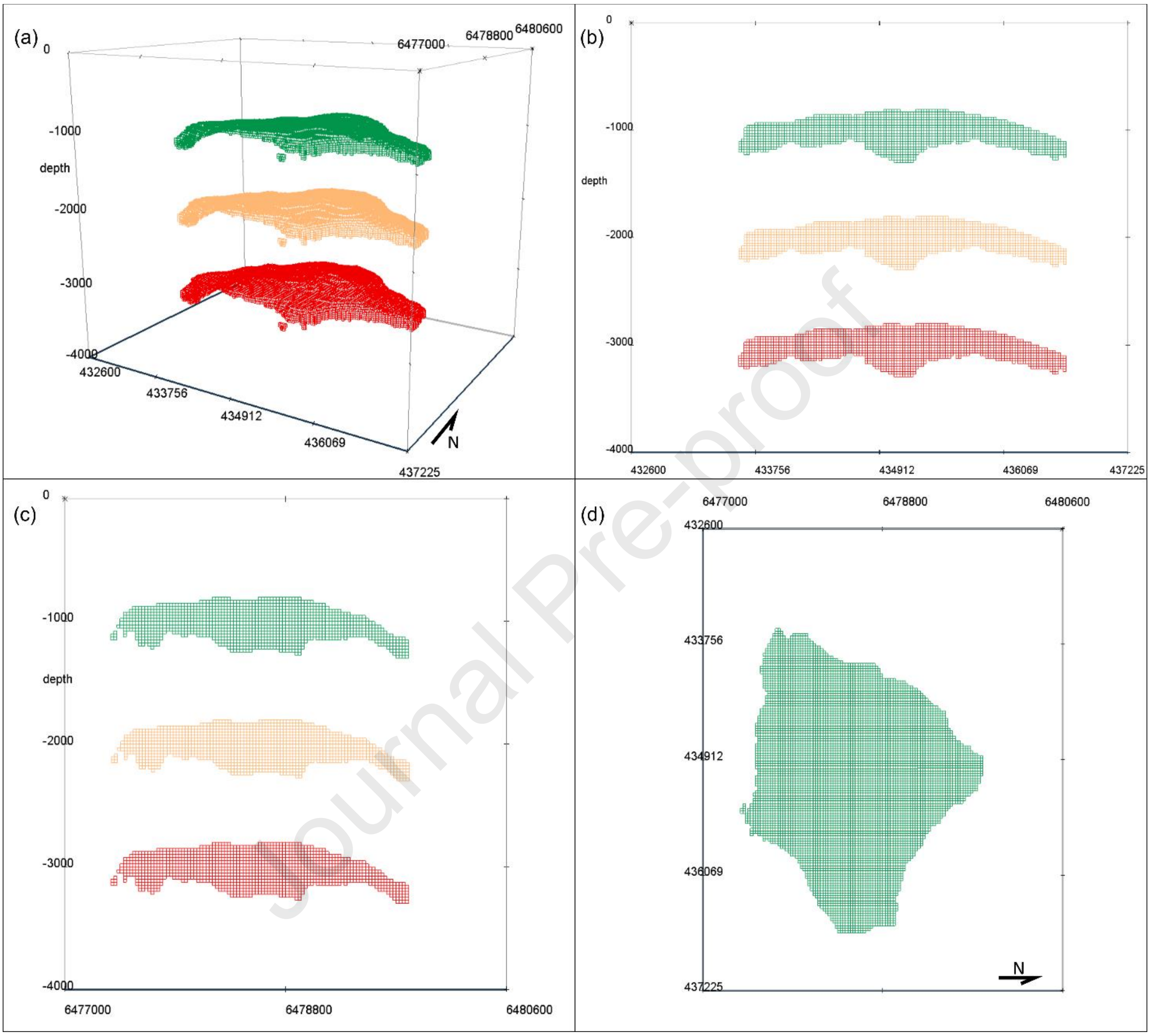

Figure 2. Volve reservoir after discretization in 25x25x25 m cells. (a) perspective view, (b) northward view, (c) westward view, (d) downward view. Red volume represents the original reservoir ranging between 2750 and 3120 m depth. Orange volume represents the same reservoir but shifted 1000 m upward and green volume was shifted 2000 m upward. Coordinates are in ED50 UTM 31N.

Results

Differential gravity anomalies retrieved from the models are shown in figures 3 and 4. In the following we report and discuss all the results.

The first model after hydrocarbon production (Fig. 3a-c) was performed assuming that the 1.47×10^9 Sm^3 volume freed by hydrocarbon production was used for carbon dioxide sequestration. In this case, we model only a complete filling of the reservoir volume and this results in Δg_z values of 12.1, 23.7 and 56 μGal with reservoir at 2750, 1750 or 750 m depth. It is worth nothing that, carbon dioxide storage results in detectable gravity signatures (Fig. 3d-f).

Next, we model the possibility that after hydrocarbon production, in case of a strong aquifer push, the reservoir is entirely or half flooded by water. In the case of a complete flooding, Δg_z is calculated between the post-production gravity and the post-flooding gravity and we observe the highest positive differential gravity signature. In fact, Δg_z ranges between 17.5 and 96.7 μGal with the reservoir at 2750 or 750 m depth, respectively. If the reservoir is located at 1750 m depth, the retrieved Δg_z is 35.7 μGal (Fig. 3g-i). If the reservoir is only half flooded, the resulting Δg_z is 8.7, 17.9 and 48.3 μGal at 2750, 1750 and 750 m depth, respectively (Fig. 3j-l). It should be noted that, if a detectability threshold for gravimeters is assumed to be 3 μGal, all the above cases would be easily observed by differential gravity measurements.

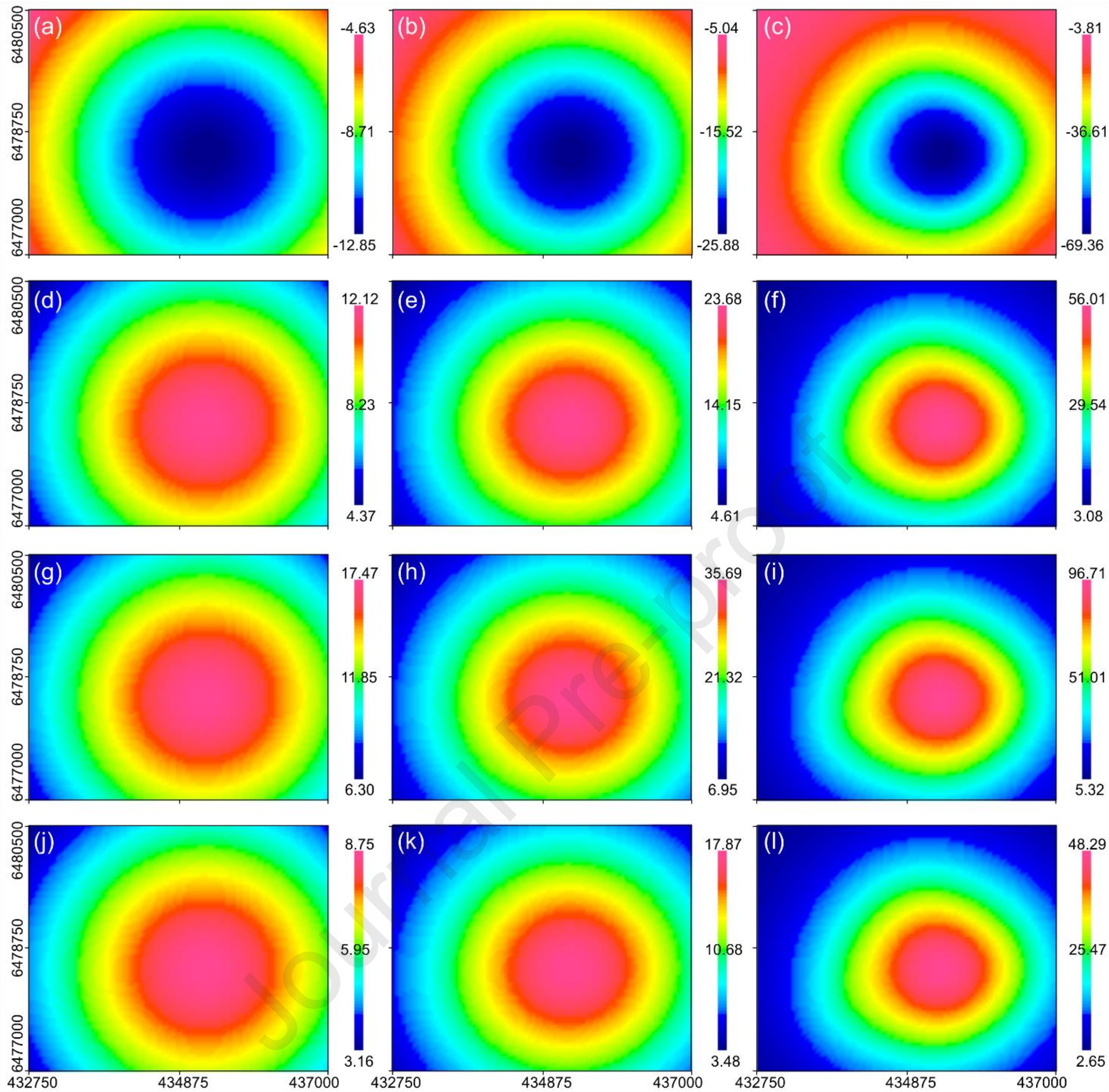

Figure 3. Differential gravity anomaly (Δg_z) maps. From left to right: reservoir at 2750, 1750 and 750 m depth. (a-c) Δg_z after primary hydrocarbon production. (d-f) Δg_z after CO_2 storage in the entire exploitable volume (1.47×10^9 Sm^3). (g-i) Δg_z after water flooding of the entire reservoir. (j-l) Δg_z after water flooding of half reservoir. All values are in μGal. In all maps the anomaly is centred over the reservoir.

In the third modelling phase, we test the scenario where the reservoir is used for hydrogen storage. In this case, prior to hydrogen injection we evaluate the possibility of injecting cushion gas to prevent eventual aquifer rise. Among the possible cushion gasses we test gravity effects of CO_2 and N_2 (Oldenburg, 2003; Feldmann *et al*. 2016) excluding the possibility that some original hydrocarbons may act as cushion. This last case, although is not uncommon, would be difficult to model due to uncertainties regarding the quantity of cushion gas required to stabilize the aquifer. For this reason, we test a scenario where 60% of the available volume ($0.88x10^9$ Sm^3) is used for cushion gas (CO_2 or N_2) and the remaining 40% is used for hydrogen storage. In the case CO_2 is used as cushion, its injection would provide detectable gravity signatures at all depths. In fact, we recover Δg_z values of 7.5, 14.7 and 34.9 μGal with reservoir at 2750, 1750 or 750 m depth (Fig. 4a-c). If N_2 is used as cushion, we recover Δg_z values of 2.7, 4.4 and 7.7 μGal with reservoir at 2750, 1750 or 750 m depth. In this case, due to the lighter cushion gas, the gravity signature would be detectable to a maximum reservoir depth of ~2500 m.

After modelling the injection of cushion gas, we model the hydrogen storage to occupy the residual 40% of the reservoir volume. In this case, the single hydrogen storage phase would not be detectable at any depth because of the low density of the injected fluid at reservoir pressure and temperature (Table 1). In fact, even in the shallow reservoir case, we recover maximum Δg_z values of 0.4 μGal, significantly below the detectability threshold of 3 μGal (Fig. 4d-f).

Finally, after injection of cushion gas we model the hydrogen withdrawal phase assuming a 50% recovery factor of the hydrogen initially stored. We are also considering the realistic possibility that in the first years of production the recovered hydrogen is impure due to mixing processes, and thus we model a 20% of the cushion gas being produced together with hydrogen in the first withdrawal cycle.

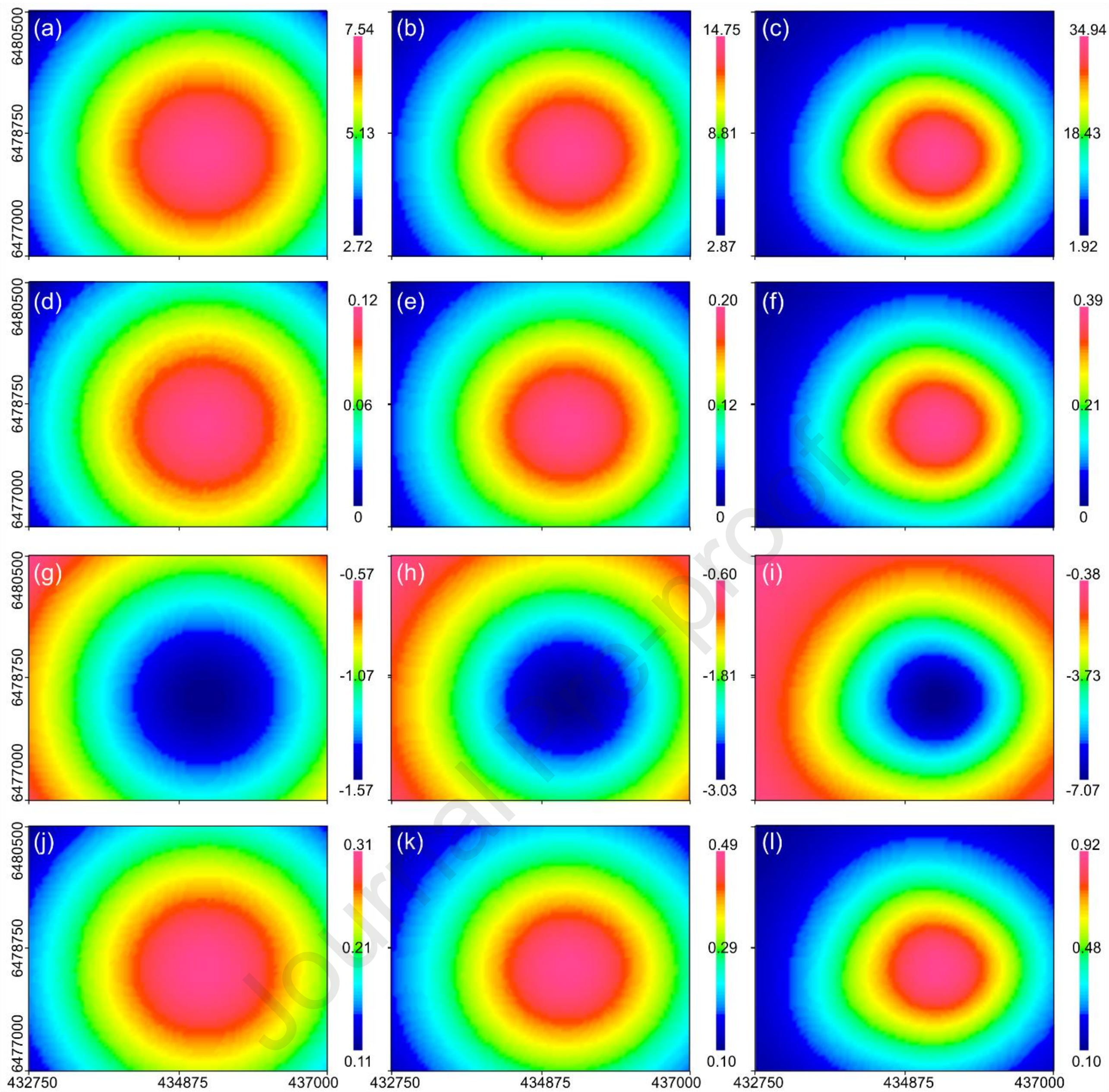

Figure 4. Differential gravity anomaly (Δg_z) maps. From left to right: reservoir at 2750, 1750 and 750 m depth. (a-c) Δg_z after CO_2 cushion gas injection in 60% of the exploitable volume. (d-f) Δg_z after hydrogen storage in 40% of the exploitable volume. (g-i) Δg_z after withdrawal of 50% of stored hydrogen and 20% of CO_2 cushion gas. (j-l) Δg_z after storage of 1.47×10^9 Sm^3 of hydrogen without cushion gas. In this figure we show only maps related to CO_2 cushion, Δg_z values retrieved using N_2 as cushion are given in the text. All values are in μGal. In all maps the anomaly is centred over the reservoir.

In the case CO_2 is used as cushion gas, the resulting Δg_z after withdrawal ranges between 1.6, 3.0 and 7.1 μGal with reservoir at 2750, 1750 or 750 m depth (Fig. 4g-i). In this case, the gravity signature would be detectable to a maximum reservoir depth of ~1750 m. On the other hand, when N_2 cushion is used, the withdrawal phase would be undetectable in the modelled depth range and likely only reservoirs within

~500 m depth would provide detectable signatures because we retrieve *Δg*Δg_z values of 0.5, 1.0 and 1.7 μGal at 2750, 1750 and 750 m depth, respectively.

Finally, we test hydrogen storage without cushion gas in the case of a reservoir without aquifer or weak-to-null aquifer push (Fig. 4j-l). Also in this case, the hydrogen-related gravity change would be undetectable at all the modelled depths even in the case of 100% recovery, because the maximum Δg_z related to a reservoir depth of 750 m is 0.9 μGal (Fig. 4l).

Discussion

In figure 5, we plot the recovered Δg_z and the modelled mass variation causing it. To increase readability of the plot, we show absolute values of maximum Δg_z, these values should be considered negative for hydrocarbon production and hydrogen withdrawal (mass loss), and positive for injection phases (mass increase). These data represent an attempt in predicting detectable levels of gravity anomalies related to fluid injection or production in a very small and deep reservoir with average porosity values of 20 ±2.5 %, relatively small thickness (~100 m) and ranging between 750 and 2750 m depth.

There are several parameters that can affect these estimates, some of them are related to the geometry and physics of the reservoir (e.g. thickness, porosity, permeability). Some others are related to chemical and physical processes that can occur in the stored fluids and affect recovery efficiency. For example, during the hydrogen withdrawal models, we assume a 50% recovery factor for the stored hydrogen. This is mostly due to eventual losses due to bacterial degradation (e.g. Kabuth *et al*. 2017) and methanogenesis via hydrogen methanation if CO_2 is used as cushion gas (Kabuth *et al*. 2017; Götz *et al*. 2016; Rönsch *et al*. 2016) whose effects in term of hydrogen loss are difficult to quantify in the storage period (weeks to months). Moreover, the 50% recovery factor for hydrogen is also accounting for eventual mixing between the hydrogen and the cushion gas that would likely affect the recoverability of the stored hydrogen. On the other hand, we model injection and production steps by only considering mass variations and this, as long as the injected or produced volume is known and the density of the fluid is well constrained, may result in reliable estimates of Δg_z.

The exploitable volume of the reservoir plays a significant role in the whole process. The Volve reservoir represents an end-member in this case because of its limited lateral extent, porosity and thickness. Thus, increasing the thickness of the reservoir will linearly affect the produced Δg_z by introducing a mass increase with strong vertical component. Conversely, enlarging the lateral extent of the reservoir will likely result in smaller increase of Δg_z due to the horizontal distribution of the mass increase.

The gravity forward models, once the differential gravity related to each step are computed, result in detectability thresholds according to modern gravimeters capabilities. Unsurprisingly, when referred to the same depth, the mass variation induced by injection/production activities is linearly affecting the gravity response, while changes in depth provide non-linear effects. Noteworthy, the proportionality between the depth to the source and the observed Δg_z is slightly less than quadratic, this is interpreted as a consequence of the geometry of the reservoir whose horizontal extent is larger than its vertical thickness (Kabirzadeh *et al.* 2020).

Gravity signatures related to N_2 being stored as cushion gas below 2500 m depth are undetectable. Conversely, storage of CO_2 is detectable down to depth of 2750 m either if it is stored alone for sequestration or if it is used as cushion gas. Withdrawal activities involving H_2 and CO_2 cushion are undetectable if the reservoir is deeper than 1750 m (Fig. 5b). Within the modelled depth range, water

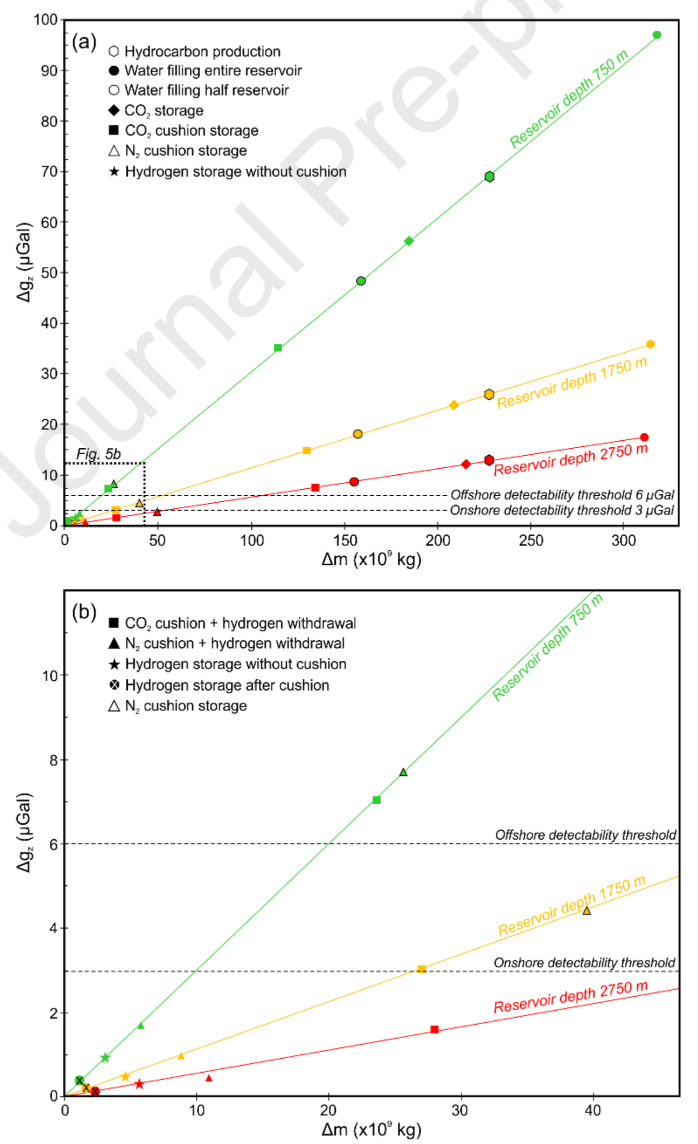

flooding always represents a detectable phenomenon, even if it affects half of the reservoir.

Figure 5. (a) Absolute values of Δg_z recovered after 3D forward models of the reservoir. Values in red denote results with reservoir depth of 2750 m, orange values denote results with reservoir depth of 1750 m and green values represent results with reservoir depth of 750 m. (b) Zoom of the plot in (a) to the area with small mass variation values (<45x10^9 kg). Squares and triangles mark only cushion gas injection in (a) and hydrogen and cushion withdrawal in (b).

In the modelling setup, we assumed that the faults surrounding the reservoir are sealed, and no fluid migration is allowed outside of the reservoir. However, if potential migration paths are known after the primary explorative phase, these can be included in the forward modelling. Otherwise, unknown migration paths can be identified and monitored by proper gravity acquisitions provided that the leaked fluid accumulates in a monitored secondary lateral reservoir and produces a detectable gravity signature. In the case of a secondary reservoir at similar depth of the primary, the plots in figure 5 allow for a first-order estimation of the masses, depending on the observed gravity signature. In the case of a secondary reservoir that is shallower than the primary – i.e. upward lateral migration of the leaked fluids, leakage detection becomes easier even for smaller masses, depending on the depth of accumulation. Alternatively, an indirect leakage estimation can be provided by repeated gravity measurements over the storage reservoir. Once the depth of the reservoir is known, the predicted gravity signature of an injection/withdrawal period can be calculated if the injected/withdrawn mass is known (Fig. 5). If a mass is lost during such period and in between two measurement campaigns, it will affect the latter gravity measurements proportionally to the leaked mass. If such effects are above the detectability threshold, the leaked mass can be estimated from the missing Δg_z component.

In the modelling, we assumed no pressure build-up at injection points and computed the models without over-pressuring the reservoir. In other words, we used the gas volume produced in the primary phase as the only available volume for storage – i.e. the exploitable volume. Eventual over-pressures, if sealing conditions and the integrity of the cap rock are preserved, will introduce an increase of the produced Δg_z linearly proportional to the increase of the injected mass.

Density of the injected fluid plays a key role in the modelling procedure and accurate pressure and temperature values at the injection point are thus fundamental to properly estimate these values. In fact, at supercritical conditions the density of the fluid may result in rapid changes even with small changes in pressure and temperature (e.g. Alnes *et al*. 2011). However, it was demonstrated that diffusion and dispersion processes act similarly on normal fluids as for supercritical fluids (Yu *et al.*, 1999; Oldenburg, 2003) so the supercritical status of the injected or withdrawn fluid will only affect its density. Considering the pressure (3.28×10^7 Pa) and temperature (106°C) at reservoir, we used fluid densities at these conditions for modelling at 2750 m depth. We corrected the density values according to pressure and thermal gradients from literature (Alnes *et al.* 2011; Volve documentation included in the dataset) at the other modelled depths (Table 1) to showcase the effects of depth, pressure and temperature on the fluid density and, in turn, on the retrievable Δg_z.

During the gas injection modelling, we assumed to be in the optimal case of no aquifer push in order to allow uniform distribution of the injected gas and avoid gravity override and viscous fingering (Feldmann *et al*. 2016). However, despite this may be the case for some real reservoirs, in some others the aquifer may partially or entirely flood the reservoir during or after primary production operations. It follows that aquifer push is another parameter that may conceal gravity effects related to fluid injection and production. In the case of strong aquifer push, the reservoir should always be filled in order to avoid water flooding. In fact, if half of the reservoir is left empty, the gravity effect produced by water flooding will completely conceal the gravity signature related to gas storage (Fig. 5). Moreover, such a scenario would also prevent any detection of possible leakage of the stored fluid. Nevertheless, reservoirs with strong aquifer push will likely represent a bad scenario for gas storage in general, because the aquifer rise can lead to unpredictable pressures of the stored gas in the long period resulting in possible leakage.

The masses injected in our simulations represent both short-term periods of injection/production (Fig. 5b) or long-term injection plans (Fig. 5a) such those modelled by Appriou et al. (2020) where a total of 150 x10^9 kg of CO_2 was injected at a 2.5 x 10^9 kg year^{-1} rate. In this latter case, the rate of injection may play a key role in the case of strong aquifer push. In fact, if the injection/sequestration of gas is slower than the aquifer rise, the available volume and in turn the injectable mass, will decay in time with obvious consequences on the retrievable Δg_z signature both considering the contribution from the stored gas and the concealing effect of the aquifer. This implies that if a long-term storage is planned over a reservoir with rising aquifer, the injection rate should consider the rising rate of the aquifer and how it will affect the storable mass in the long-term.

Noise sources affecting the detectability threshold

Among the phenomena affecting the time-lapse gravity measurements there is a list of geophysical sources that can produce significant effects or even conceal the monitored signal. In fact, our 3 μGal detectability threshold is achievable and representative only if all the potential noise sources are addressed and eventually corrected. A compelling discussion about all the noise sources is provided in Van Camp et al. (2017) and references therein. In the following we briefly discuss the most relevant for the application we tested in this work.

Local-scale and regional-scale sources of gravity noise can be distinguished. Among the local ones, we already modelled and discussed reservoir aquifer but did not mention the case of ground water mass variations above the reservoir. The noise from this source can last decades and show maximum amplitudes of tens of μGals. Similarly, subsidence-related signals can potentially conceal gravity signatures similar to those modelled in this work with periods spanning from months to decades. Moreover, also tides can provide similar noise with even higher amplitudes. However, all these noise sources can be properly addressed by accurate piezometric monitoring of eventual ground water masses (e.g. Kim *et al.* 2015 and references therein), precise levelling of gravity stations, and accurate tidal models. The first task always represents a good practice in reservoir fields, while the tidal modelling and station levelling are always required in gravity data acquisition and processing and it all reduces to the accuracy of the instruments used to address these tasks. Among the regional-scale noise sources listed by Van Camp et al. (2017) that are capable of generating noise amplitudes higher than those modelled in this work, mass displacements related to pre-seismic and post-seismic events can cause pore pressure changes and deformation inside and around the reservoir. Therefore, these parameters should be monitored over production or storage reservoirs as the accuracy of such monitoring will directly affect the reliability of the time-lapse gravity measurements. Given the porosity and thickness of the modelled reservoir, we assumed negligible ground deformation. Despite this might be the case, there are chances that surface deformation occurs following injection of large volumes in confined reservoirs (Kabirzadeh *et al.*, 2017a; 2017b). In such cases, the magnitude of the free-air effect related to ground deformation can be calculated (Kabirzadeh *et al.*, 2017b; 2020) and removed from the gravity signal.

Conclusions

The Volve field, given its exploitable volume and depth, represents an end-member in the lower term of reservoir classification based on size because it can be considered a very small and deep reservoir. Thus, the differential gravity signatures observed in this work, together with the retrieved detectability thresholds, represent a minimum base of the gravity effects induced by fluid storage and withdrawal in real reservoirs. Nevertheless, some general considerations can be drawn from the modelling above.

The most relevant parameters affecting differential gravity investigations over reservoirs are represented by the depth of the reservoir, aquifer push, exploitable volume, and densities of the fluids at reservoir conditions. The combination of these parameters, together with the accuracy of the monitoring techniques, drives the recoverability of reliable differential gravity signatures. Moreover, the depth of the reservoir, the aquifer push and available volumes – i.e. the volume obtained during primary production, are well-known when a reservoir has been discovered, parametrized and exploited for years using seismic, borehole and laboratory data. Density of the injected fluid is a parameter that needs careful attention, particularly when pressures and temperatures at reservoir allows supercritical conditions that can lead to abrupt changes in fluid density.

Water flooding of the reservoir results in differential gravity anomalies that are always observable even at significant depths and in very small reservoirs due to the strong mass anomaly it produces. In fact, water flooding may conceal gravity signatures related to other sources such gas storage or withdrawal even if only half of the reservoir is flooded. Similarly, operations involving CO_2 result in differential gravity anomalies that are always detectable unless they provide small mass changes (< $50x10^9$ kg) at significant depths (> 1750 m).

Due to the small introduced mass changes, gravity changes related to hydrogen injection or withdrawal are undetectable at this reservoir size. Only the production of hydrogen coupled with CO_2 cushion gas would be detectable from very small reservoirs at maximum depth of ~1750 m. The ideal conditions to detect differential gravity signatures during storage or withdrawal operations involving only hydrogen are given by shallow (<1000 m) and thick (>> 100 m) reservoirs.

Finally, the data shown in figure 5 can provide valid support to estimate mass variations related to the observed Δg_z. In fact, in the case of a suspected leakage of the reservoir, if the spilled fluid generates a detectable gravity signal after accumulation in a secondary monitored reservoir with known depth, the mass lost from the reservoir can be estimated from the observed Δg_z . Alternatively, the monitoring of the primary reservoir may provide indirect estimates of the mass lost between two surveys if the masses injected and/or withdrawn during the cycle are known.

Data availability

The data used in this work are available from sources in the public domain: https://www.equinor.com/en/how-and-why/digitalisation-in-our-dna/volve-field-data-village-download.html

Acknowledgements

We warmly thank four anonymous reviewers for their constructive and insightful reviews. Constructive comments from the editor Luigi Tosi are also warmly acknowledged. We warmly thanks Equinor for making available the Volve dataset. This work was supported by funds to PM from the Department of Engineering and Geology of the Chieti-Pescara University.

References

Alnes, H., Eiken, O., and Stenvold, T. (2008). Monitoring gas production and CO_2 injection at the Sleipner field using time-lapse gravimetry. Geophysics 73, WA155–WA161. doi: 10.1190/1.2991119.

Alnes, H., Eiken, O., Nooner, S., Sasagawa, G., Stenvold, T., and Zumberge, M. (2011). Results from sleipner gravity monitoring: updated density and temperature distribution of the CO_2 plume. Energy Procedia 4, 5504–5511. doi: 10.1016/j.egypro.2011.02.536

Appriou, D., Bonneville, A., Zhou, Q. and Gasperikova, E. (2020). Time-lapse gravity monitoring of CO2 migration based on numerical modeling of a faulted storage complex, International Journal of Greenhouse Gas Control, Volume 95, 102956, https://doi.org/10.1016/j.ijggc.2020.102956.

Dressel, I., Barckhausen, U., and Heyde, I. (2018). A 3D gravity and magnetic model for the Entenschnabel area (German North Sea). Int. J. Earth Sci. 107, 177–190. doi: 10.1007/s00531-017-1481-x

Eiken, O., Stenvold, T., Zumberge, M., Alnes, H., and Sasagawa, G. (2008). Gravimetric monitoring of gas production from the Troll feld. Geophysics 73, WA149–WA154.

Eiken, O., Zumberge, M. A., and Sasagawa, G. S. (2000). “Gravity monitoring of offshore gas reservoirs,” in Proceedings of the 70th Annual International Meeting, SEG, Expanded Abstracts (Tulsa, OK: SEG) 431–434

Elliott, E. J., and Braun, A. (2016). Gravity monitoring of 4D fluid migration in SAGD reservoirs – forward modelling. CSEG Rec. 41, 16–21. https://csegrecorder.com/articles/view/gravity-monitoring-of-4d-fluid-migration-in-sagd-reservoirs

Fedi, M., Cella, F., D’Antonio, M., Florio, G., Paoletti, V., and Morra, V. (2018). Gravity modelling finds a large magma body in the deep crust below the gulf of Naples, Italy. Sci. Rep. 8:8229. doi: 10.1038/s41598-018-26346-z

Feldmann, F., Hagemann, B., Ganzer, L. and Panfilov, M. (2016). Numerical simulation of hydrodynamic and gas mixing processes in underground hydrogen storages. Environmental Earth Science 75:1165 doi: 10.1007/s12665-016-5948-z.

Ferguson, J., Klopping, F., Chen, T., Seibert, J., Hare, J., and Brady, J. (2008). The 4D microgravity method for waterflood surveillance: Part III – 4D absolute microgravity surveys at Prudhoe Bay. Alaska. Geophysics 73, WA163–WA171.

Ferguson, J. F., Chen, T., Brady, J. L., Aiken, C. L. V., and Seibert, J. E. (2007). The 4D microgravity method for waterflood surveillance II — gravity measurements for the Prudhoe Bay reservoir, Alaska. Geophysics 72, I33–I43. doi: 10.1190/1.2435473.

Gasperikova, E. and Hoversten, G. M. (2008). Gravity monitoring of CO_2 movement during sequestration: Model studies. Geophysics 73(6):WA105–WA112. https ://doi.org/10.1190/1.29858 23

Goto, H., Ishido, T. and Sorai, M. (2020). Numerical study of reservoir permeability effects on gravity changes associated with CO2 geological storage: implications for gravimetric monitoring feasibility. Greenhouse Gases-Science and Technology 10: 557-566.

Götz, M., Lefebvre, J., Mörs, F., McDaniel Koch, A., Graf, F., Bajohr, S., Reimert, R. and Kolb, T. (2016) Renewable power-to-gas: a technological and economic review. Renewable Energy 85:1371–1390. doi:10.1016/j.renene.2015.07.066

Hagrey, S. A., Kohn, D., Wiegers, C. E., Schafer, D. and Rabbel. W. (2014). Feasibility study for geophysical monitoring renewable gas energy compressed in pore storages. Journal of Geology and Geosciences 3:5, doi: 10.4172/2329-6755.1000169.

Hare, J. L., Ferguson, J. F., Aiken, C. L. V., and Brady, J. L. (1999). The 4-D microgravity method for waterflood surveillance: a model study for the Prudhoe Bay reservoir, Alaska. Geophysics 64, 78–87. doi: 10.1190/1.1444533

Jacob, T., Bayer, R., Chery, J., and Le Moigne, N. (2010). Time-lapse microgravity surveys reveal water storage heterogeneity of a karst aquifer. J. Geophys. Res. 115, 1–18. doi: 10.1029/2009JB006616.

Jacob, T., Rohmer, J. and Manceau J-C. (2016). Using surface and borehole time-lapse gravity to monitor CO2 in saline aquifers: a numerical feasibility study. Greenh. Gas. Sci. Technol. 6:34–54. https ://doi.org/10.1002/ghg.1532

Kabuth, A., Dahmke, A., Beyer, C., Bilke, L., Dethlefsen, F., et al. (2017). Energy storage in the geological subsurface: dimensioning, risk analysis and spatial planning: the ANGUS+ project. Environmental Earth Science 76:23 doi: 10.1007/s12665-016-6319-5.

Kabirzadeh, H., Kim, J.W. and Sideris, M.G. (2017a). Micro-gravimetric monitoring of geological CO2 reservoirs. Int. J. Greenh. Gas Control 56: 187–219.

Kabirzadeh, H., Sideris, M.G., Shin, Y. J. and Kim, J.W. (2017b). Gravimetric Monitoring of Confined and Unconfined Geological CO2 Reservoirs. Energy Procedia 114, 3961-3968.

Kabirzadeh, H., Kim, J.W., Sideris, M.G. and Vatankhah, S. (2020). Analysis of surface gravity and ground deformation responses of geological CO2 reservoirs to variations in CO2 mass and density and reservoir depth and size. Environ Earth Sci 79, 163. https://doi.org/10.1007/s12665-020-08902-x

Kim, J.W., Neumeyer, J., Kao, R. and Kabirzadeh, H. (2015). Mass balance monitoring of geological CO2 storage with a superconducting gravimeter—a case study. J. Appl. Geophys. https://doi.org/10.1016/j.jappgeo.2015.01.003

Krahenbuhl, R.A., Martinez, C., Li, Y. and Flanagan, G. (2015). Time-lapse monitoring of CO2 sequestration: A site investigation through integration of reservoir properties, seismic imaging, and borehole and surface gravity data. Geophysics 80(2):WA15–WA24

Mancinelli, P., Pauselli, C., Minelli, G., and Federico, C. (2015). Magnetic and gravimetric modelling of the central Adriatic region. J. Geodynamics 89, 60–70. doi: 10.1016/j.jog.2015.06.008

Mancinelli, P., Porreca, M., Pauselli, C., Minelli, G., Barchi, M. R., and Speranza, F. (2019). Gravity and magnetic modelling of central Italy: insights into the depth extent of the seismogenic layer. Geochem. Geophys. Geosyst. 20, 2157–2172.doi: 10.1029/2018GC008002.

Mancinelli, P. (2020). Four Dimensional Gravity Forward Model in a Deep Reservoir. Frontiers in Earth Sciences 8:285. doi: 10.3389/feart.2020.00285.

Mancinelli, P., Pauselli, C., Fournier, D., Fedi, M., Minelli, G., and Barchi, M. R. (2020). Three dimensional gravity local inversion across the area struck by the 2016–2017 seismic events in central Italy. J. Geophys. Res. 125:e2019JB018853. doi: 10.1029/2019JB018853.

NIST (2016). Thermophysical properties of fluid systems. https://webbook.nist.gov/chemistry/fluid/

Oldenburg, C. M. (2003). Carbon dioxide as cushion gas for natural gas storage. Energy Fuels 17(1): 240-246.

Olesen, O., Ebbing, J., Gellein, J., Kihle, O., Myklebust, R., Sand, M., et al. (2010). Gravity Anomaly Map, Norway and Adjacent Areas. Scale 1:3 Million. Trondheim: Geological survey of Norway. https://www.ngu.no/en/publikasjon/gravity-anomaly-map-norway-and-adjacent-areas-scale-13-mill

Pfeiffer, W. T., al Hagrey, S. A., Kohn, D., Rabbel, W. and Bauer, S. (2016). Porous media hydrogen storage at a synthetic, heterogeneous field site: numerical simulation of storage operation and geophysical monitoring. . Environmental Earth Science 75:1177 doi: 10.1007/s12665-016-5958-x.

Pudlo, D., Ganzer, L., Henkel, S., Kühn, M., Liebscher A., et al. (2013). The H2STORE project: hydrogen underground storage – a feasible way in storing electrical power in geological media? In: Hou, M.Z., Xie, H. & Were, P. (eds.): Clean Energy Systems in the Underground: Production, Storage and Conversion. Springer Series in Geomechanics and Geoengineering. Springer, Berlin, Heidelberg. https://doi.org/10.1007/978-3-642-37849-2_31

Rönsch, S., Schneider, J., Matthischke, S., Schlüter, M., Götz, M., Lefebvre, J., Prabhakaran, P. and Bajohr, S. (2016). Review on methanation from fundamentals to current projects. Fuel 166:276–296. doi:10.1016/j.fuel.2015.10.111

Van Camp, M., de Viron, O., Watlet, A., Meurers, B., Francis, O., and Caudron, C. (2017). Geophysics from terrestrial time-variable gravity measurements. Rev. Geophys. 55, 938–992. doi: 10.1002/2017RG000566

Volve data village webpage: https://www.equinor.com/en/how-and-why/digitalisation-in-our-dna/volve-field-data-village-download.html last visited on January 27, 2021.

Wilkinson, M., Mouli-Castillo, J., Morgan, P. and Eid, R. (2017). Time-lapse gravity surveying as a monitoring tool for CO2 storage. Int. J. Greenh. Gas Control 60:93–99.

Yu, D., Jackson, K. and Harmon, T. C. (1999). Dispersion and Diffusion in Porous Media under Supercritical Conditions. Chem. Eng. Sci. 54, 357-367.

Highlights for the manuscript entitled "Gravity effects of fluid storage and withdrawal in a reservoir from 3D forward modelling " by Paolo Mancinelli

- We test the recoverability of differential gravity anomalies produced by fluid storage or withdrawal over a real reservoir
- We model different evolutive scenarios after reservoir primary production: carbon dioxide storage, carbon dioxide or nitrogen cushion gas injection, hydrogen injection and withdrawal
- We evaluate effects of reservoir depth on the recovered gravity signatures by repeating the calculations between 750 and 2750 m depth
- Results provide reference values for gravity signatures related to fluid storage in the worst-case scenario of a deep (~2750 m) and thin (~100 m) reservoir.

Declaration of interests

☒ The authors declare that they have no known competing financial interests or personal relationships that could have appeared to influence the work reported in this paper.

☐The authors declare the following financial interests/personal relationships which may be considered as potential competing interests: